Theoretical efficiency limit and realistic losses of indoor organic and perovskite photovoltaics [Invited]

Xinlu Liu (刘鑫璐)[†], Ruiyu Tian (田睿宇)[†], Zedong Xiong (熊泽栋), Yang Liu (刘 洋), and Yinhua Zhou (周印华)[*]

Wuhan National Laboratory for Optoelectronics, Huazhong University of Science and Technology, Wuhan 430074, China

Indoor organic and perovskite photovoltaics (PVs) have been attracting great interest in recent years. The theoretical limit of indoor PVs has been calculated based on the detailed balance method developed by Shockley–Queisser. However, realistic losses of the organic and perovskite PVs under indoor illumination are to be understood for further efficiency improvement. In this work, the efficiency limit of indoor PVs is calculated to 55.33% under indoor illumination (2700 K, 1000 lux) when the bandgap (E_g) of the semiconductor is 1.77 eV. The efficiency limit was obtained on the basis of assuming 100% photovoltaic external quantum efficiency (EQE_{PV}) when $E \geq E_g$, there was no nonradiative recombination, and there were no resistance losses. In reality, the maximum EQE_{PV} reported in the literature is 0.80–0.90. The proportion of radiative recombination in realistic devices is only 10^{-5}–10^{-2}, which causes the open-circuit voltage loss (ΔV_{loss}) of 0.12–0.3 V. The fill factor (FF) of the indoor PVs is sensitive to the shunt resistance (R_{sh}). The realistic losses of EQE_{PV}, nonradiative recombination, and resistance cause the large efficiency gap between the realistic values (excellent perovskite indoor PV, 32.4%; superior organic indoor PV, 30.2%) and the theoretical limit of 55.33%. In reality, it is feasible to reach the efficiency of 47.4% at 1.77 eV for organic and perovskite photovoltaics under indoor light (1000 lux, 2700 K) with $V_{OC} = 1.299$ V, $J_{SC} = 125.33$ μA/cm^2, and FF = 0.903 when $EQE_{PV} = 0.9$, $EQE_{EL} = 10^{-1}$, $R_s = 0.5$ Ω cm^2, and $R_{sh} = 10^4$ kΩ cm^2.

Keywords: theoretical efficiency limit; realistic efficiency losses; organic photovoltaics; perovskite photovoltaics; indoor photovoltaics.

DOI: 10.3788/COL202321.120031

1. Introduction

Indoor photovoltaics (IPVs) based on the organic and organic–inorganic halide perovskite semiconductors are attracting attention due to their easy fabrication, good mechanical flexibility, and great application potential to power the Internet of Things (IoTs)[1–3]. Different from the one-sun illumination (air mass 1.5G, 100 mW/cm^2), whose spectrum covers 250 to 2500 nm, the spectrum of the indoor light source is mainly in the visible region of 400–760 nm. The detailed balance between the light harvest and thermalization loss in the cells under indoor illumination for a semiconductor with a specific bandgap (E_g) is different from the case under one-sun illumination. The power conversion efficiencies (PCEs) of 20%–30% for organic IPVs[1,4–10] and 30%–40% for perovskite IPVs[3,11–13] have been reported. These are much higher than those PCE values of cells under one-sun illumination: the PCE record is over 19% for organic PVs[14–17] and over 25% for perovskite PVs[18] under one-sun illumination.

The Shockley–Queisser (SQ) efficiency limit[19,20] of single-junction solar cells under one-sun illumination has now become

widely acknowledged and is an important fundamental theory of PV research. For IPVs, similar calculations on the efficiency limit of IPVs have been performed based on the detailed balance method developed by Shockley–Queisser (SQ). The calculated efficiency limit of the IPVs is 50%–60% at the E_g of 1.8–1.9 eV[21–23]. The limit values slightly change according to different spectra of indoor light. The literature reports that the highest efficiencies of indoor organic PVs and perovskite PVs are 33% (concentrating indoor light to 20,000 lux)[6] and 36.36% (under indoor light of 1000 lux, measured at the Chinese National Photovoltaic Industry Measurement and Testing Center)[11], respectively. These values are still far behind the calculated values. However, understanding the realistic losses of the efficiency and comparing this with the calculated theoretical limit of IPVs has not been discussed.

In this work, we analyze the realistic losses of the efficiency of indoor organic and perovskite PVs, comparing these realistic efficiency losses to the theoretical limit. The calculated theoretical efficiency limit was obtained based on assuming 100% photovoltaic external quantum efficiency (EQE_{PV}) when $E \geq E_g$, there was no nonradiative recombination, and there were no

resistance losses. In reality, the maximum EQE_{PV} at different wavelengths reported from the literature is 0.80–0.90[5,6,11,13,24–28] (mainly due to optical losses). The portion of radiative recombination [typically by measuring the electroluminescent quantum efficiency (EQE_{EL})] in realistic devices is only $10^{-5} - 10^{-2}$[7–9,11,28], which causes the open-circuit voltage loss (ΔV_{loss}) of 0.12–0.3 V. In addition, the fill factor (FF) is sensitive to shunt resistance (R_{sh}) while being less sensitive to series resistance (R_{s}). Thus, these realistic losses in the EQE_{PV}, the EQE_{EL}, and the R_{sh} cause the large efficiency gap between the realistic values and the theoretical limit. Accordingly, strategies to further increase the efficiency of IPVs include enhancing the EQE_{PV}, suppressing the nonradiative combination to increase the EQE_{EL}, and increasing the R_{sh}.

2. Results and Discussion

The methods for the calculation are included in Supplementary Material 1. The MATLAB codes are provided in Supplementary Material 2. Figures 1(a)–1(d) show the maximum PCE, FF, open-circuit voltage (V_{OC}), and short-circuit current density (J_{SC}) at different E_{g} ranging from 1.2 to 2.5 eV. Four different indoor light sources are included, i.e., two different incident light spectra, whose color temperatures are 2700 K and 4651 K, respectively, and two different light intensities (500 and 1000 lux). Figure 1(f) shows the indoor light spectra from the light-emitting diodes (LEDs). The light intensity of the 2700 K, 1000 lux LED is 310.102 μW/cm², while the light

intensity of the 4651 K, 1000 lux LED is 299.193 μW/cm². As shown in Fig. 1(a) and Table 1, the PCE limit is 55.33% (under 1000 lux) and 54.54% (under 500 lux) under 2700 K light when the E_{g} is 1.771 eV. Under 4651 K indoor illumination, the PCE limit is 53.93% (under 1000 lux) and 53.20% (under 500 lux) when the E_{g} is 1.85 eV. The maximum FF and V_{OC} curves at different E_{g} are almost identical under four different light sources [Figs. 1(b) and 1(c)]. The maximum FF and V_{OC} monotonically increase as the E_{g} increases. Figure 1(d) shows the maximum J_{SC} of the devices at different E_{g}. J_{SC} under 1000 lux illumination is twice as high as that under 500 lux illumination. Under 1000 lux, the maximum J_{SC} of the devices is about 150 μA/cm² for 2700 K light and 133 μA/cm² for 4651 K. Since the 1000 lux and 2700 K illumination is the commonly used indoor illumination for research[9,29–31], we hereafter use this light source for the analysis of the realistic losses. At the E_{g} of 1.77 eV, the cells under 2700 K and 1000 lux can ideally have an efficiency limit of 55.33%, with an FF of 0.907, a V_{OC} of 1.356 V, and a J_{SC} of 139.53 μA/cm² (Table 1).

The above efficiency limit of IPVs was calculated on the basis of the following assumptions. (1) All photons with energy higher than or equal to the E_{g} of the semiconductor are fully absorbed, and photons with energy lower than the E_{g} are not absorbed. The EQE_{PV} is a step function. The EQE_{PV} is 1 at $E \geq E_{\text{g}}$, and 0 at $E < E_{\text{g}}$. (2) Each photon absorbed produces only one electron-hole pair. (3) There is no nonradiative recombination but only radiative recombination in the devices. (4) The device emits the spectrum as a blackbody at room temperature (300 K).
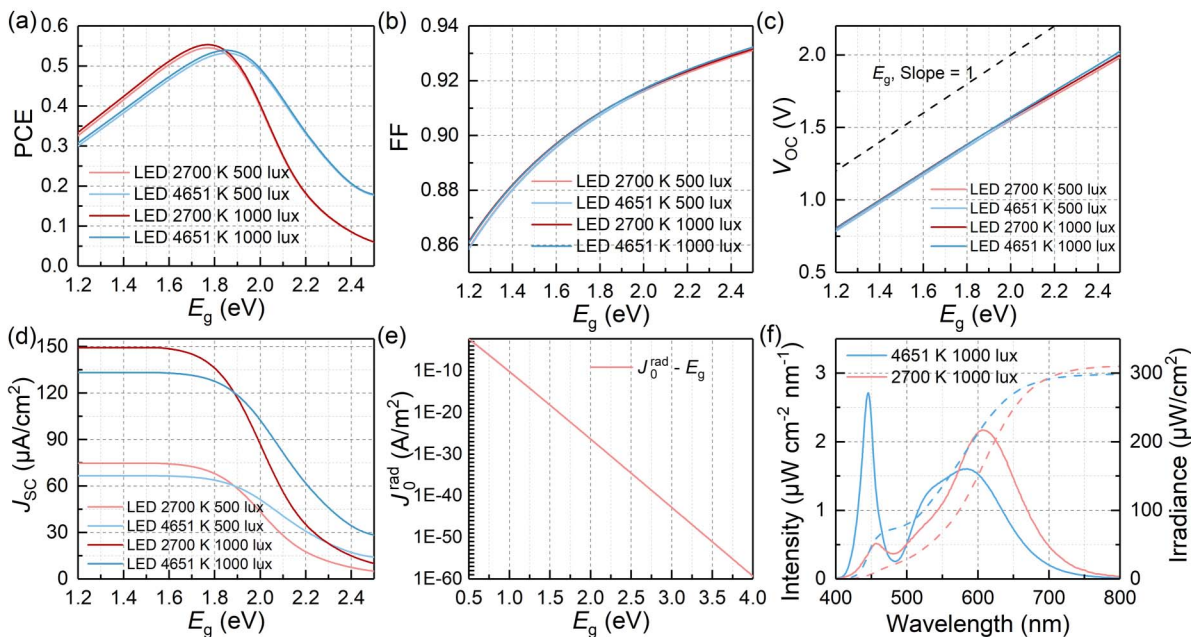
Fig. 1. Theoretical efficiency limit of indoor photovoltaics. (a)–(d) The theoretical limit of PCE, FF, V_{OC}, and J_{SC} of IPVs as a function of the band gap (E_{g}) under different indoor conditions at 300 K. (e) The calculated J_0 (J_0^{rad}, radiative recombination only at 300 K) as a function of E_{g}. (f) The spectra of indoor light used for the calculation (2700 and 4651 K at 1000 lux).

Table 1. Theoretical Efficiency Limit and Corresponding Photovoltaic Data of Indoor Photovoltaics under Four Different Illumination Conditions: Two Different Spectra (2700 and 4651 K) and Two Different Light Intensities (500 and 1000 lux).

Color Temperature	Irradiance (μW/cm^2)	Illuminance (lux)	E_g (eV)	V_{OC} (V)	J_{SC} (μA/cm^2)	FF	PCE
2700 K	310.102	1000	1.771	1.356	139.53	0.907	55.33%
	155.051	500	1.771	1.338	69.76	0.906	54.54%
4651 K	299.193	1000	1.851	1.430	123.90	0.911	53.93%
	149.596	500	1.853	1.415	61.83	0.910	53.20%

The theoretical PCE limit of IPVs is 55.33% under 2700 K, 1000 lux illumination, while the realistic PCE of perovskite and organic IPVs are far lower. Understanding these realistic losses is important for further enhancing the efficiency of IPVs. The PCE is determined by the product of the J_{SC}, the V_{OC}, and the FF. Each of the three parameters will cause losses of the PCE.

For the loss of J_{SC}, in the calculation, it is assumed that the EQE_{PV} is 100% in the spectral region with $E \geq E_g$. In reality, not all photons with energy exceeding E_g can be fully absorbed and converted into free charge carriers. The EQE_{PV} of the device is not constant at 100%. The light reflection, the transmittance of transparent electrode, and the charge carrier recombination are the origin losses of EQE_{PV} and J_{SC}. Figure 2(a) shows the EQE_{PV} of two high-efficiency perovskite[12] and organic[28] IPVs reported in the literature. The perovskite photovoltaics can deliver high EQE_{PV} of about 90% and be quite constant in the indoor spectral region[11,24,26,27]. The organic IPVs can deliver EQE_{PV} in the range of 80%–90% but is not constant due to their small film thickness[5,6,28]. That suggests that the practical J_{SC} generally causes 10%–15% loss compared with the theoretical J_{SC}. Figure 2(b) shows that limit of the J_{SC} at different E_g when EQE_{PV} is 0.7, 0.8, 0.9, and 1.0 under the 2700 K, 1000 lux illumination. Under such illumination, the maximum J_{SC} is 149.3, 134.4, 119.5, and 104.5 μA/cm^2 for the EQE_{PV} of 1.0, 0.9, 0.8, and 0.7 at the E_g of 1.2 eV, respectively. To achieve high PCE of the IPVs, it is important to further enhance the EQE_{PV} to a high value approaching 1 in the entire indoor spectral region.

For the loss of V_{OC}, the open-circuit voltage loss (ΔV_{loss}) mainly includes two parts of radiative and nonradiative recombination, as shown in Eq. (1),

$$\Delta V_{loss} = \frac{E_g}{e} - V_{OC} = \Delta V^{rad} + \Delta V^{non\text{-}rad}, \qquad (1)$$

where ΔV^{rad} and $\Delta V^{non\text{-}rad}$ represent the loss caused by radiative recombination and nonradiative recombination, respectively. ΔV^{rad} is associated with the temperature of the devices and E_g of semiconductors. Every photovoltaic device working under temperatures higher than 0 K will emit and cause the voltage loss. The ΔV^{rad} is calculated with Eq. (2)[32,33], which is correlated with the J_{SC} and the J_0^{rad} [Fig. 1(e)],

$$\Delta V^{rad} = \frac{E_g}{e} - \frac{nkT}{e} \ln\left(\frac{J_{SC}}{J_0^{rad}} + 1\right), \qquad (2)$$

where e represents the elementary charge; n is the ideality factor of the p-n junction, and its value is 1 here; k is the Boltzmann constant; T is the absolute temperature; and J_0^{rad} represents the reverse saturation current density caused by radiative recombination. Under indoor illumination, the ΔV^{rad} is the difference between the E_g and the V_{OC} when the $EQE_{EL} = 1$ and the $EQE_{PV} = 1$, included in Fig. 3, which is the larger, in the range of 0.4–0.5 V. It is higher than the ΔV^{rad} under one-sun illumination (typically 0.2–0.3 V[3]). That is because the J_{SC} of the cells under indoor illumination is 2–3 orders of magnitude
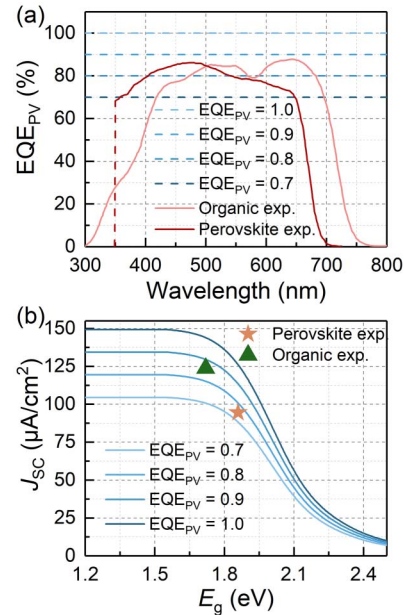
Fig. 2. Realistic loss analysis of J_{SC}. (a) The EQE_{PV} spectra of recently reported high-performance perovskite[12] and organic[28] solar cells. The blue dash lines indicate the positions of the EQE_{PV} of 0.7–1. (b) The integrated J_{SC} as a function of the different EQE_{PV} spectra, where EQE_{PV} is a step function; $EQE_{PV} = 0.7, 0.8, 0.9,$ or 1 ($E \geq E_g$); and $EQE_{PV} = 0$ ($E < E_g$). The asterisk and triangle represent the J_{SC} of the recently reported high-performance indoor (1000 lux) perovskite[12] and organic[28] photovoltaics, respectively.
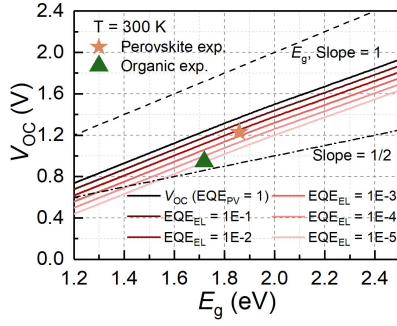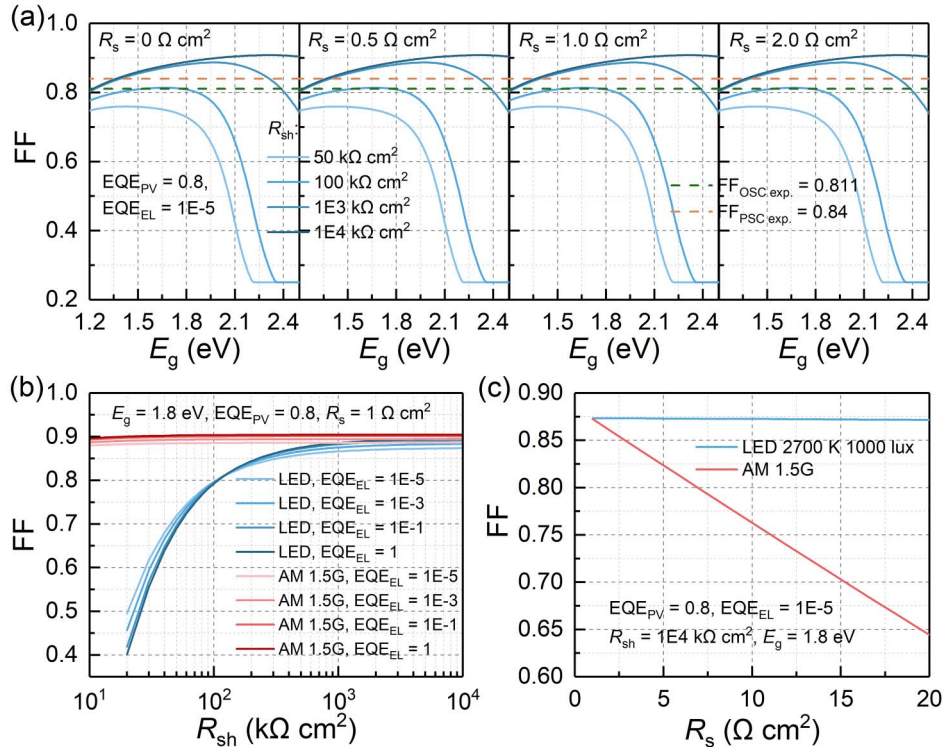
Fig. 3. Realistic loss analysis of the V_{OC}. Plots of the V_{OC} limit as a function of E_g, under different nonradiative recombination. The black solid line represents the V_{OC} with the loss caused by only radiative recombination (without non-radiative recombination). The difference between the dash line (slope = 1) and black solid line is the loss caused by radiative recombination (ΔV^{rad}). The asterisk and triangle represent recently reported high-performance indoor (1000 lux) perovskite[12] and organic[28] photovoltaics, respectively.

lower than that under one-sun illumination. Figure S1 (Supplementary Material 1) shows that the higher temperature of the cells would result in the stronger radiation of the black-body and a higher ΔV^{rad}. According to the calculation, when the temperature rises by 5 K, the ΔV^{rad} would increase by about 0.01 V.

In addition to the loss caused by radiative recombination, the loss caused by nonradiative recombination ($\Delta V^{non\text{-}rad}$) is also critical. The $\Delta V^{non\text{-}rad}$ can be calculated by the following equation[33,34]:

$$\Delta V^{non\text{-}rad} = -\frac{nkT}{e}\ln(\text{EQE}_{EL}), \qquad (3)$$

where the EQE_{EL} represents electroluminescent quantum efficiency of the device and suggests the proportion of radiative recombination to the total recombination. As shown in Fig. 3, increasing the EQE_{EL} can effectively reduce the $\Delta V^{non\text{-}rad}$, resulting in the improvement of the V_{OC}. The $\Delta V^{non\text{-}rad}$ is reduced to 60 meV when the EQE_{EL} increases by one order of magnitude. Table S1 (Supplementary Material 1) shows the values of $\Delta V^{non\text{-}rad}$ when the EQE_{EL} changes from 10^{-1} to 10^{-5}. At present, the outstanding organic active layer materials can achieve EQE_{EL} of around 10^{-3} (such as PBDB-TF:GS-ISO[9]), which results in a small $\Delta V^{non\text{-}rad}$ of 0.17 V. For perovskite solar cells, the EQE_{EL} can be much higher, in the range of about $10^{-2}-10^{-1}$ [12,35]. Thus, the $\Delta V^{non\text{-}rad}$ of the perovskite PVs is lower than that of the organic PVs. The calculation of ΔV^{rad} and $\Delta V^{non\text{-}rad}$ is based on the step function of the EQE_{PV} with a value of 1 when $E \geq E_g$. In reality, the EQE_{PV} generally has a sloped tail rather than a step function, and the
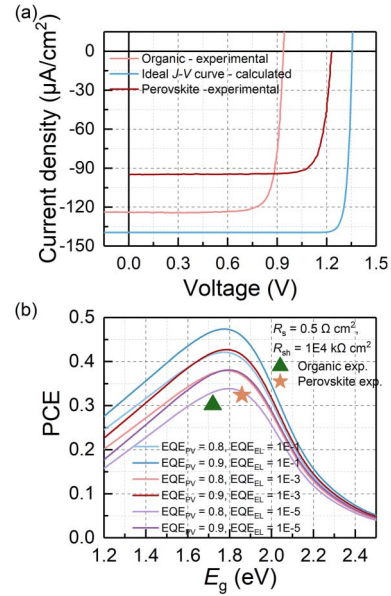

Fig. 4. Realistic loss analysis of the FF. (a) The FF of the IPVs as a function of E_g when R_s is 0, 0.5, 1.0, and 2.0 Ω cm^2 and R_{sh} is 50, 100, 10^3, and 10^4 kΩ cm^2, respectively. The dash lines represent the FF of recently reported high-performance indoor (1000 lux) perovskite[12] (0.84) and organic[28] (0.811) photovoltaics, respectively. (b) The FF as a function of the resistance of the devices under indoor (2700 K, 1000 lux) illumination (R_{sh}) and (c) one-sun (AM 1.5G, 100 mW cm^{-2}) illumination (R_s). Different EQE_{EL} conditions were considered.

EQE_PV value is not constantly 1. That will cause additional voltage loss. Based on the experimental data, this voltage loss can be as low as 0.066 V for organic[28] and perovskite[11] PVs. Thus, we do not include this part of the voltage loss into the Fig. 3.

For the realistic loss of the FF, the FF is influenced by the series resistance (R_s) and the shunt resistance (R_{sh}). In the calculation of the efficiency limit, the R_s is zero and the R_{sh} is infinity. In reality, the drop of the FF as a function of the R_s and the R_{sh} is shown in Fig. 4(a). The FF of the IPVs is very sensitive to the R_{sh}. When the R_{sh} is high, 10^4 kΩ cm², the FF monotonically increases as a function of E_g. When the R_{sh} is lower, the trend of the FF as a function of E_g is changed, and the value of the FF is lower. This is because the current under indoor illumination is low, on the order of μA/cm². If the R_{sh} is not high enough, then the shunt current will be high and significantly reduce the output power (P_{out}). The behavior of the FF (as a function of R_s and R_{sh}) under indoor illumination is different from that under one-sun illumination. As shown in Figs. 4(b) and 4(c), the FF of the device under one-sun illumination is quite constant when the R_{sh} changes from 20 to 300 kΩ cm², while the FF of the device under indoor illumination increases rapidly from 0.4 to 0.86. On the contrary, the FF of the device under one-sun illumination is sensitive to the R_s, which drops from 0.87 down to 0.64 when the R_s changes from 0.1 to 20 Ω cm², while the FF of the device under indoor illumination is constantly high, 0.87, when the R_s changes from 0.1 to 20 Ω cm² [Fig. 4(c)]. In addition, the nonradiative recombination (EQE_EL) also slightly influences the FF. When the EQE_EL increases from 10^{-5} to 1, the FF increases from 0.87 to 0.90 when the R_s is 1 Ω cm² and the R_{sh} is 10^4 kΩ cm². Thus, a large R_{sh} is important for the FF of IPVs.

Figure 5(a) shows the comparison of the J-V characteristics between the theoretical limit (V_{OC} = 1.356 V, J_{SC} = 139.53 μA/cm², FF = 0.907, and PCE = 55.33% at the E_g of 1.77 eV) and the realistic organic[28] (V_{OC} = 0.943 V, J_{SC} = 123.8 μA/cm², FF = 0.811, and PCE = 30.2% at E_g of 1.72 eV) and perovskite[12] (V_{OC} = 1.23 V, J_{SC} = 94.54 μA/cm², FF = 0.84, and PCE = 32.41% at E_g of 1.86 eV) IPVs. The J_{SC}, the V_{OC}, and the FF are all lower than the theoretical limit, which caused the large gap between the realistic efficiencies and the theoretical limit. Based on the above discussion, it can be known that the efficiency loss is due to the loss of the EQE_PV, the EQE_EL, and the R_{sh}. Figure 5(b) shows the plots of the PCE as a function of E_g with different EQE_PV and EQE_EL. The R_{sh} was set as 10^4 kΩ cm² since the FF saturates at this value, as shown in Fig. 4(b). The following information can be obtained: (1) the optimum E_g is 1.77–1.80 eV to achieve the highest PCE for IPVs, and (2) the EQE_PV and the EQE_EL could significantly change the PCE of the IPVs. When the EQE_PV = 0.9 and the EQE_EL = 10^{-1}, the PCE can reach a high value of 47.39% at 1.77 eV (V_{OC}= 1.299 V, J_{SC} = 125.33 μA/cm², and FF = 0.903, Table 2). When the EQE_PV = 0.8 and the EQE_EL = 10^{-5}, the PCE is lower of 33.86% (V_{OC} = 1.080 V, J_{SC} = 109.45 μA/cm², and FF = 0.888). The asterisk and triangle in the figure correspond

Fig. 5. Realistic loss analysis of the PCE. (a) The theoretical and experimental J-V characteristics of the IPVs. The blue line represents the theoretical limit (V_{OC} = 1.356 V, J_{SC} = 139.53 μA/cm², FF = 0.907, and PCE = 55.33% at E_g of 1.77 eV). The pink and red lines represent the realistic organic[28] (V_{OC} = 0.943 V, J_{SC} = 123.8 μA/cm², FF = 0.811, and PCE = 30.2% at E_g of 1.72 eV) and perovskite[12] (V_{OC} = 1.23 V, J_{SC} = 94.54 μA/cm², FF = 0.84, and PCE = 32.4% at E_g of 1.86 eV) solar cells' curves, respectively. (b) The PCE limit as a function of E_g with different EQE_PV and EQE_EL (R_s = 0.5 Ω cm² and R_{sh} = 10^4 kΩ cm²). The asterisk and triangle represent recently reported high-performance indoor (1000 lux) perovskite[12] and organic[28] solar cells, respectively.

to the PCE values of the reported organic[28] and perovskite[12] IPVs.

To improve the PCE of the realistic IPVs, it is important to increase the EQE_PV and the EQE_EL, while maintaining the R_{sh} over 10^4 kΩ cm². The J_{SC} (EQE_PV) could be improved by choosing high-performance active layers, reducing the light reflection, and increasing the transmittance of transparent electrode. The

Table 2. Calculated Photovoltaic Parameters of IPVs with Different Values of EQE_PV and EQE_EL [a].

EQE_PV	EQE_EL	E_g (eV)	V_{OC} (V)	J_{SC} (μA/cm²)	FF	PCE
0.8	10^{-1}	1.774	1.299	110.40	0.903	42.12%
0.9	10^{-1}	1.774	1.299	125.33	0.903	**47.39%**
0.8	10^{-3}	1.784	1.189	110.47	0.896	37.96%
0.9	10^{-3}	1.784	1.189	124.28	0.896	42.71%
0.8	10^{-5}	1.794	1.080	109.45	0.888	**33.86%**
0.9	10^{-5}	1.794	1.080	123.14	0.888	38.09%

[a]R_s and R_{sh} were 0.5 Ω cm² and 10^4 kΩ cm² for Calculation.

V_{OC} (EQE$_{EL}$) could be enhanced by suppressing the nonradiative recombination via defect passivation or improving the crystallinity of the active layer. Currently, the maximum EQE$_{EL}$ reported in the literature is around 10^{-3} for organic PVs[9,28] and $10^{-2} - 10^{-1}$ for perovskite PVs[12,35]. In the future, it is desirable for the EQE$_{EL}$ to be enhanced to over 10^{-1}. As a result, it is feasible for the PCE to reach a high value of 47.39% with an EQE$_{PV}$ of 0.9 and an EQE$_{EL}$ of 10^{-1} at the E_g of 1.77 eV.

3. Conclusions

In this work, we have discussed the theoretical efficiency limit and realistic losses of indoor photovoltaics. The power conversion efficiency limit of indoor photovoltaics is 55.33% (indoor condition: 1000 lux, 2700 K light) when the E_g of the active layer is 1.77 eV. The efficiency limit is based on assuming 100% EQE$_{PV}$ when $E \geq E_g$, no nonradiative recombination (EQE$_{EL}$ = 1), infinity shunt resistance, and zero series resistance. In reality, the losses of the EQE$_{PV}$, the EQE$_{EL}$, and the shunt resistance cause the large gap between the efficiency of the realistic devices and the theoretical limit. The efficiency of the PV devices under indoor illumination is sensitive to the R_{sh}, while being sensitive to the R_s under one-sun illumination. Combining the highest parameters reported in the literature of R_{sh} = 10^4 kΩ cm^2, EQE$_{PV}$ = 0.9, and EQE$_{EL}$ = 10^{-1}, it could be feasible that the PCE reaches a value of 47.39% at 1.77 eV for organic and perovskite IPVs. To realize this value, it is important to reduce the optical loss and nonradiative recombination and increase the R_{sh} by reducing the leakage current.

Acknowledgement

†These authors contributed equally to this work.

References

1. Y. Cui, L. Hong, and J. Hou, "Organic photovoltaic cells for indoor applications: opportunities and challenges," ACS Appl. Mater. Interfaces **12**, 38815 (2020).
2. L. Xie, W. Song, J. Ge, B. Tang, X. Zhang, T. Wu, and Z. Ge, "Recent progress of organic photovoltaics for indoor energy harvesting," Nano Energy **82**, 105770 (2021).
3. Z. Guo, A. K. Jena, and T. Miyasaka, "Halide perovskites for indoor photovoltaics: the next possibility," ACS Energy Lett. **8**, 90 (2023).
4. Y. Cui, Y. Wang, J. Bergqvist, H. Yao, Y. Xu, B. Gao, C. Yang, S. Zhang, O. Inganäs, F. Gao, and J. Hou, "Wide-gap non-fullerene acceptor enabling high-performance organic photovoltaic cells for indoor applications," Nat. Energy **4**, 768 (2019).
5. F. Bai, J. Zhang, A. Zeng, H. Zhao, K. Duan, H. Yu, K. Cheng, G. Chai, Y. Chen, J. Liang, W. Ma, and H. Yan, "A highly crystalline non-fullerene acceptor enabling efficient indoor organic photovoltaics with high EQE and fill factor," Joule **5**, 1231 (2021).
6. W. Wang, Y. Cui, T. Zhang, P. Bi, J. Wang, S. Yang, J. Wang, S. Zhang, and J. Hou, "High-performance organic photovoltaic cells under indoor lighting enabled by suppressing energetic disorders," Joule **7**, 1067 (2023).
7. P. Bi, J. Ren, S. Zhang, T. Zhang, Y. Xu, Y. Cui, J. Qin, and J. Hou, "Suppressing energetic disorder enables efficient indoor organic photovoltaic cells with a PTV derivative," Front Chem. **9**, 684241 (2021).
8. P. Bi, J. Ren, S. Zhang, J. Wang, Z. Chen, M. Gao, Y. Cui, T. Zhang, J. Qin, Z. Zheng, L. Ye, X. Hao, and J. Hou, "Low-cost and high-performance poly (thienylene vinylene) derivative donor for efficient versatile organic photovoltaic cells," Nano Energy **100**, 107463 (2022).
9. P. Bi, S. Zhang, J. Ren, Z. Chen, Z. Zheng, Y. Cui, J. Wang, S. Wang, T. Zhang, J. Li, Y. Xu, J. Qin, C. An, W. Ma, X. Hao, and J. Hou, "A high-performance nonfused wide-bandgap acceptor for versatile photovoltaic applications," Adv. Mater. **34**, 2108090 (2022).
10. Z. Ding, R. Zhao, Y. Yu, and J. Liu, "All-polymer indoor photovoltaics with high open-circuit voltage," J. Mater. Chem. A **7**, 26533 (2019).
11. C. Zhang, C. Liu, Y. Gao, S. Zhu, F. Chen, B. Huang, Y. Xie, Y. Liu, M. Ma, Z. Wang, S. Wu, R. E. I. Schropp, and Y. Mai, "Br vacancy defects healed perovskite indoor photovoltaic modules with certified power conversion efficiency exceeding 36%," Adv. Sci. **9**, 2204138 (2022).
12. Z. Guo, S. Zhao, N. Shibayama, A. Kumar Jena, I. Takei, and T. Miyasaka, "A universal method of perovskite surface passivation for CsPbX$_3$ solar cells with V_{OC} over 90% of the S-Q limit," Adv. Funct. Mater. **32**, 2207554 (2022).
13. Z. Li, J. Zhang, S. Wu, X. Deng, F. Li, D. Liu, C. C. Lee, F. Lin, D. Lei, C.-C. Chueh, Z. Zhu, and A. K. Y. Jen, "Minimized surface deficiency on wide-bandgap perovskite for efficient indoor photovoltaics," Nano Energy **78**, 105377 (2020).
14. L. Zhu, M. Zhang, J. Xu, C. Li, J. Yan, G. Zhou, W. Zhong, T. Hao, J. Song, X. Xue, Z. Zhou, R. Zeng, H. Zhu, C. C. Chen, R. C. I. MacKenzie, Y. Zou, J. Nelson, Y. Zhang, Y. Sun, and F. Liu, "Single-junction organic solar cells with over 19% efficiency enabled by a refined double-fibril network morphology," Nat. Mater. **21**, 656 (2022).
15. Z. Chen, H. Yao, J. Wang, J. Zhang, T. Zhang, Z. Li, J. Qiao, S. Xiu, X. Hao, and J. Hou, "Restrained energetic disorder for high-efficiency organic solar cells via a solid additive," Energy Environ. Sci. **16**, 2637 (2023).
16. J. Wang, Y. Wang, P. Bi, Z. Chen, J. Qiao, J. Li, W. Wang, Z. Zheng, S. Zhang, X. Hao, and J. Hou, "Binary organic solar cells with 19.2% efficiency enabled by solid additive," Adv. Mater. **35**, 2301583 (2023).
17. X. Xu, W. Jing, H. Meng, Y. Guo, L. Yu, R. Li, and Q. Peng, "Sequential deposition of multicomponent bulk heterojunctions increases efficiency of organic solar cells," Adv. Mater. **35**, 2208997 (2023).
18. J. Park, J. Kim, H. S. Yun, M. J. Paik, E. Noh, H. J. Mun, M. G. Kim, T. J. Shin, and S. I. Seok, "Controlled growth of perovskite layers with volatile alkylammonium chlorides," Nature **616**, 724 (2023).
19. W. Shockley and H. J. Queisser, "Detailed balance limit of efficiency of p-n junction solar cells," J. Appl. Phys. **32**, 510 (1961).
20. S. Rühle, "Tabulated values of the Shockley–Queisser limit for single junction solar cells," Sol. Energy **130**, 139 (2016).
21. J. K. W. Ho, H. Yin, and S. K. So, "From 33% to 57%–an elevated potential of efficiency limit for indoor photovoltaics," J. Mater. Chem. A **8**, 1717 (2020).
22. M. Freunek, M. Freunek, and L. M. Reindl, "Maximum efficiencies of indoor photovoltaic devices," IEEE J. Photovolt. **3**, 59 (2013).
23. A. S. Teran, J. Wong, W. Lim, G. Kim, Y. Lee, D. Blaauw, and J. D. Phillips, "AlGaAs photovoltaics for indoor energy harvesting in mm-scale wireless sensor nodes," IEEE Trans. Electron Devices **62**, 2170 (2015).
24. M. Li, C. Zhao, Z. K. Wang, C. C. Zhang, H. K. H. Lee, A. Pockett, J. Barbé, W. C. Tsoi, Y. G. Yang, M. J. Carnie, X. Y. Gao, W. X. Yang, J. R. Durrant, L. S. Liao, and S. M. Jain, "Interface modification by ionic liquid: a promising candidate for indoor light harvesting and stability improvement of planar perovskite solar cells," Adv. Energy Mater. **8**, 1801509 (2018).
25. R. Singh, M. Parashar, S. Sandhu, K. Yoo, and J.-J. Lee, "The effects of crystal structure on the photovoltaic performance of perovskite solar cells under ambient indoor illumination," Sol. Energy **220**, 43 (2021).
26. S. Kim, H. Oh, G. Kang, I. K. Han, I. Jeong, and M. Park, "High-power and flexible indoor solar cells via controlled growth of perovskite using a greener antisolvent," ACS Appl. Energy Mater. **3**, 6995 (2020).

27. N. Talbanova, T. Komaricheva, L. O. Luchnikov, G. Ermolaev, V. Kurichenko, D. S. Muratov, A. Arsenin, I. S. Didenko, V. Volkov, I. V. Badurin, M. V. Ryabtseva, N. T. Vagapova, D. Saranin, and A. Di Carlo, "Color-temperature performance of perovskite solar cells under indoor illumination," Sol. Energy Mater. Sol. Cells **254**, 112284 (2023).

28. T. Zhang, C. An, Y. Xu, P. Bi, Z. Chen, J. Wang, N. Yang, Y. Yang, B. Xu, H. Yao, X. Hao, S. Zhang, and J. Hou, "A medium-bandgap nonfullerene acceptor enabling organic photovoltaic cells with 30% efficiency under indoor artificial light," Adv. Mater. **34**, 2207009 (2022).

29. S. Hwang and T. Yasuda, "Indoor photovoltaic energy harvesting based on semiconducting π-conjugated polymers and oligomeric materials toward future IoT applications," Polym. J. **55**, 297 (2023).

30. Y. Cui, H.-F. Yao, Y. Xu, P.-Q. Bi, J.-Q. Zhang, T. Zhang, L. Hong, Z.-H. Chen, Z.-X. Wei, X.-T. Hao, and J.-H. Hou, "100 cm^2 organic photovoltaic cells with 23% efficiency under indoor illumination," Chin. J. Polym. Sci. **40**, 979 (2022).

31. Y. Cui, H. Yao, T. Zhang, L. Hong, B. Gao, K. Xian, J. Qin, and J. Hou, "1 cm^2 organic photovoltaic cells for indoor application with over 20% efficiency," Adv. Mater. **31**, 1904512 (2019).

32. J. Liu, S. Chen, D. Qian, B. Gautam, G. Yang, J. Zhao, J. Bergqvist, F. Zhang, W. Ma, H. Ade, O. Inganäs, K. Gundogdu, F. Gao, and H. Yan, "Fast charge separation in a non-fullerene organic solar cell with a small driving force," Nat. Energy **1**, 16089 (2016).

33. J. Yao, T. Kirchartz, M. S. Vezie, M. A. Faist, W. Gong, Z. He, H. Wu, J. Troughton, T. Watson, D. Bryant, and J. Nelson, "Quantifying losses in open-circuit voltage in solution-processable solar cells," Phys. Rev. Appl. **4**, 014020 (2015).

34. U. Rau, "Reciprocity relation between photovoltaic quantum efficiency and electroluminescent emission of solar cells," Phys. Rev. B **76**, 085303 (2007).

35. Z. Liu, C. Duan, F. Liu, C. C. S. Chan, H. Zhu, L. Yuan, J. Li, M. Li, B. Zhou, K. S. Wong, and K. Yan, "Perovskite bifunctional diode with high photovoltaic and electroluminescent performance by holistic defect passivation," Small **18**, 2105196 (2022).